WILEY VCH

RESEARCH ARTICLE

Enantioselective and Regiodivergent Synthesis of Propargyl- and Allenylsilanes through Catalytic Propargylic C−H Deprotonation

Jin Zhu, Hengye Xiang, Hai Chang, James C. Corcoran, Ruiqi Ding, Yue Xia, Peng Liu* and Yi-Ming Wang[a]*

[a] J. Zhu, H. Xiang, H. Chang, J. C. Corcoran, R. Ding, Y. Xia, Prof. Dr. P. Liu, Prof. Dr. Y.-M. Wang
Department of Chemistry
University of Pittsburgh
Pittsburgh, PA 15260 (USA)
E-mail: pengliu@pitt.edu
ym.wang@pitt.edu

Supporting information for this article is given via a link at the end of the document.

Abstract: We report a highly enantioselective intermolecular C−H bond silylation catalyzed by a phosphoramidite-ligated iridium catalyst. Under reagent-controlled protocols, propargylsilanes resulting from C(sp^3)−H functionalization, as well the regioisomeric and synthetically versatile allenylsilanes, could be obtained with excellent levels of enantioselectivity and good to excellent control of propargyl/allenyl selectivity. In the case of unsymmetrical dialkyl acetylenes, good to excellent selectivity for functionalization at the less-hindered site was also observed. A variety of electrophilic silyl sources (R_3SiOTf and R_3SiNTf_2), either commercial or *in situ*-generated, were used as the silylation reagents, and a broad range of simple and functionalized alkynes, including aryl alkyl acetylenes, dialkyl acetylenes, 1,3-enynes, and drug derivatives were successfully employed as substrates. Detailed mechanistic experiments and DFT calculations suggest that an η^3-propargyl/allenyl Ir intermediate is generated upon π-complexation-assisted deprotonation and undergoes outer-sphere attack by the electrophilic silylating reagent to give propargylic silanes, with the latter step identified as the enantiodetermining step.

Introduction

Well-defined propargylic stereocenters serve as indispensable building blocks for stereoselective synthesis and are found in a number of bioactive molecules.[1,2] Widely applied approaches for their construction include the substitution of propargylic alcohol derivatives and the nucleophilic addition of metal acetylides to electrophiles.[3] As an alternative, the enantioselective transformation of propargylic C(sp^3)−H bonds constitutes a direct but underdeveloped approach for obtaining stereodefined α-functionalized alkynes (Scheme 1A). The radical-based enantioselective Kharasch−Sosnovsky oxygenation represents an early example of such a transformation, though it remains limited to a narrow range of alkyne substrates.[4] More recently, Guosheng Liu and coworkers reported a successful propargylic cyanation based on chiral Cu catalysts, which is believed to involve radical and organocopper intermediates.[5] Under similar reaction conditions, the Liu group also reported the regioselective synthesis of chiral allenyl nitriles from alkynes by propargylic C−H functionalization with concomitant 1,3-rearrangement.[6] Although both propargylic and allenic nitriles could be prepared in high yield and enantioselectivity using this approach, the regiochemical outcome of this process appears to be largely controlled by substrate structure. Metal nitrene or carbene insertion is another powerful tool for C−H functionalization, and these methods are particularly effective for intramolecular propargylic amination or alkylation reactions.[7] While intermolecular transformations remain rare, enzymatic methods have been successfully applied toward the synthesis of propargylic amines and alcohols.[8]

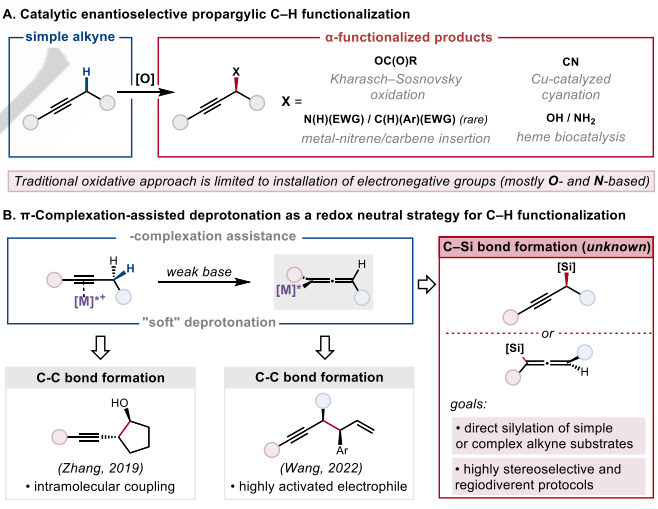

Scheme 1. Asymmetric propargylic functionalization

Given the oxidative nature of these transformations, the incorporation of a wider array of electron-neutral or electron-rich carbon- or heteroatom-based functional groups through propargylic C–H functionalization poses an ongoing challenge. Thus, the development of a generic strategy for enantioselective functionalization of the propargylic position of alkynes using electrophilic reagents under non-redox conditions would be highly desirable. We posited that a *π-complexation-assisted deprotonation strategy* for the generation of a chiral allenylmetal

reagent from an alkyne (Scheme 1B, top left) could enable the desired enantioselective propargylic functionalization.[9] Liming Zhang and coworkers previously demonstrated the utility of this approach using bifunctional Au/Brønsted base catalysts for intramolecular coupling of alkyne and aldehydes,[10] while more recently, our group reported an intermolecular propargylic allylation in the presence of an Ir catalyst (Scheme 1B, bottom left).[11] The successful development of this highly stereo- and regioselective system for propargylic C–H allylation using allylic ethers as allylic cation equivalents led us to explore the feasibility using other easily accessible electrophilic reagents for introducing heteroatom-based functional groups (Scheme 1B, right).

Chiral compounds containing silicon are of significant interest to drug and agrochemical discovery efforts.[12] Enantioenriched organosilicon compounds, especially propargyl- and allenylsilanes, are versatile synthetic intermediates that can be transformed stereospecifically into a range of other functionalized products.[13] Although a variety of selective and efficient methods for the synthesis of enantioenriched alkyl silanes are available,[14] only a few methods deliver stereodefined propargyl- and allenylsilanes (Scheme 2A).[15] Importantly, the requirement for prefunctionalized alkyne derivatives and nucleophilic silyl sources (e.g., hydrides and boryls) as starting materials impose practical limitations on the scope of these transformations. On the other hand, the direct C(sp^3)–H silylation constitutes a straightforward way to introduce a silicon atom. However, enantioselective strategies remain underexplored and seldom reported.[16] Multiple transition metals have proven to be effective towards non-enantioselective C(sp^3)–H silylation at elevated temperatures.[17] By contrast, the direct enantioselective functionalization of a prochiral C(sp^3) center through metal-catalyzed silylation is, to the best of our knowledge, limited to the intramolecular desymmetrization of substrates bearing pendant cyclopropyl or *gem*-dimethyl moieties with hydrosilanes (Scheme 2B).[18]

Given the broad availability and accessibility of alkynes, we felt that the alternative approach of using silyl electrophiles as reagents in the context of a deprotonative strategy facilitated by transition metal coordination would give rise to broadly applicable C–H functionalization protocols for the preparation of synthetically versatile enantioenriched propargyl- and allenylsilanes. However, silyl electrophiles, especially the widely available silyl chlorides and triflates, are rarely used for C–Si bond formation in catalytic organometallic processes.[19] In the absence of bromide or iodide additives for generation of a more reactive silyl halide reagent *in situ*, there is only a single report (a Ni-catalyzed silyl-Heck reaction) of a transition metal catalyzed C–Si bond forming protocol employing silyl triflate reagents.[20] This rarity can be largely attributed to the high Si–O bond dissociation energy of these species (Scheme 2C). In addition, the choice of reagent would need to be compatible with the cationic metal catalyst and amine base used for deprotonation.

In spite of these potential obstacles, we disclose herein the successful implementation of this strategy. In this Article, we describe the development of enantioselective and regiodivergent protocols for the synthesis of propargylic and allenic silanes from several classes of simple or functionalized alkynes, including aryl-alkyl, alkenyl-alkyl, and alkyl-alkyl acetylenes. Silyl triflates and bistriflimides, either commercially available or prepared *in situ*, are effectively intercepted by nucleophilic allenyliridium intermediates in the silylation process (Scheme 2C). Experimental mechanistic studies and density-functional theory calculations revealed that the reaction proceeds through a unique catalytic cycle involving C–H deprotonation and outer-sphere silylation of an organoiridium species, a process previously unknown for iridium catalysis.

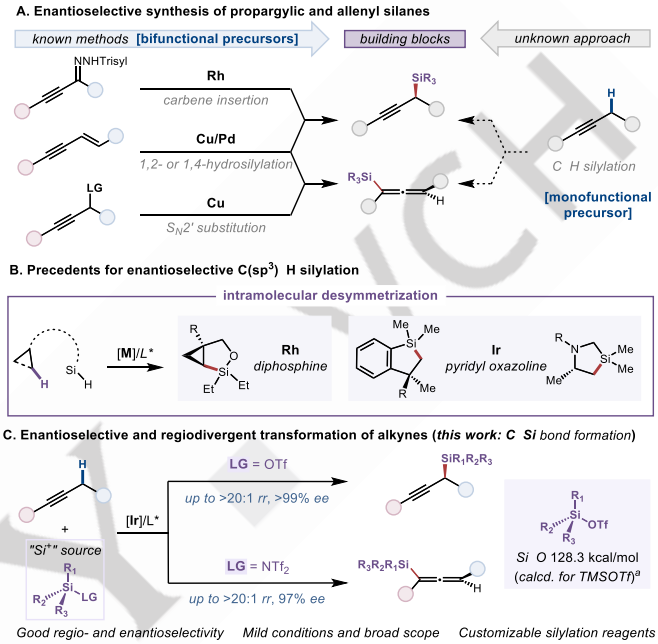

Scheme 2. C–H silylation for enantioselective propargyl- and allenylsilane synthesis. [a] DFT calculation performed at the ωB97x-D/6-311+G(d,p)/SMD(DCE)//B3LYP-D3(BJ)/6-31G(d) level of theory.

Results and Discussion

In our initial studies, 1-phenyl-1-butyne (**1a**) was selected as the model alkyne substrate for propargylic silylation. We tested the reactivity of triethylsilyl triflate (TESOTf, **2a**) as the silylation reagent employing an array of chiral bidentate phosphorus ligands, including phosphoramidites and diphosphines. The desired product was obtained with excellent enantioselectivity though in modest yield with phosphoramidite ligand $\mathbf{L_1}$. A 2:1 ratio of chiral ligand to metal was found to give considerably better catalytic activity compared to a 1:1 ratio. In contrast to previously reported Ir-catalyzed C(sp^3)−H silylation reactions,[17] the hydrosilane Et_3SiH was found to be ineffective (Table 1, entry 1). The use of triethylsilyl chloride as the reagent likewise did not afford the product (entry 2).[19d] However, when a prestirred mixture of Et_3SiH and TfOH was used as the reagent,[21] the silylation product was formed in high yield and excellent enantioselectivity (entry 4), indicating that silyl triflate formed *in situ* was an effective reagent. Silanes with other leaving group were also tested as potential silylation reagents. Notably, the switch to silyl bistriflimide not only produced propargylsilane product, but also led to the formation of the isomeric allenylsilane

in a 1:2.1 ratio (entry 6). Further optimization of reagent ratios and the incorporation of $LiNTf_2$ as an additive led to additional improvements in the regioselectivity (entry 7, 8). Among a range of organic and inorganic bases examined, 2,2,6,6-tetramethylpiperidine (TMPH) was found to be uniquely effective. Finally, control experiments omitting iridium source, ligand, and base one at a time demonstrated the necessity of each of these components in this transformation (see the Supporting Information).

Table 1. Optimization of the Ir-catalyzed silylation [a]

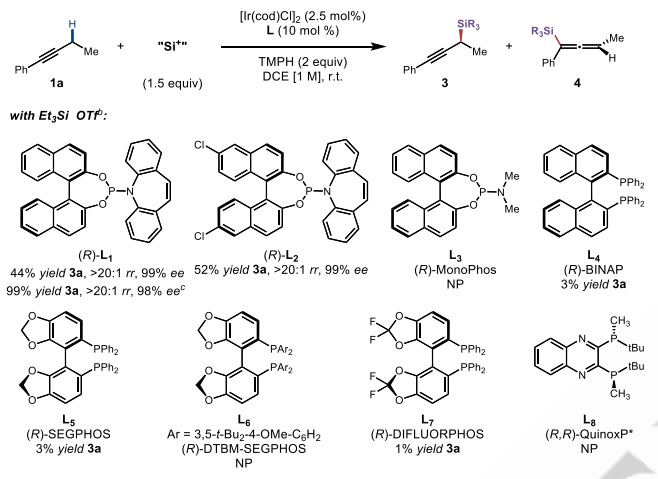

Entry[c]	"Si+" reagents	% yield	rr (**3**:**4**)	% ee
1	Et_3SiH	NP	ND	ND
2	Et_3SiCl	NP	ND	ND
3[d]	Et_3SiOTf	99 (91)	>20:1	98 (97)
4[e]	Et_3SiH + HOTf	95	>20:1	98
5	Me_3SiOMs	NP	ND	ND
6	Me_3SiNTf_2	64	1:2.1	98
7[f]	Me_3SiNTf_2	91	1:8.3	97
8[f, g]	Me_3SiNTf_2	82 (73)	1:9.2	97
9[f, h]	Me_3Si(allyl) + $HNTf_2$	61	1:7.6	96

[a] On 0.1 mmol scale. Yields were determined by ^1H NMR spectroscopy of the crude reaction mixture, using 1,1,2,2-tetrachloroethane as the internal standard, DCE: 1,2-dichloroethane, NP: no desired product observed, ND: not determined. Enantiomeric excess (ee) of major regioisomer was determined by HPLC with chiral stationary phase. [b] $[Ir(cod)Cl]_2$ 2.5 mol %, **L** 5 mol % were used. [c] $[Ir(cod)Cl]_2$ 2.5 mol %, **L** 10 mol % were used. [d] Yield and enantioselectivity of isolated product (0.2 mmol scale, 2 M) in parentheses. [e] Et_3SiH and TfOH were mixed and stirred for 5 min before adding to the reaction mixture. [f] TMPH 3 equiv, $TMSNTf_2$ 3 equiv. [g] $LiNTf_2$ 50 mol % as additive. Yield and enantioselectivity of isolated product (0.2 mmol scale, 1 M) in parentheses. [h] Trimethylallylsilane and Tf_2NH were mixed and stirred for 45 min before adding to the reaction mixture.

With optimized reaction conditions established, the scope of the transformation was investigated. Using commercially available trimethylsilyl (TMS) and triethylsilyl (TES) triflates as the silyl sources, a diverse collection of alkyl aryl acetylenes were first examined (Table 2). Substrates bearing electron withdrawing and donating aryl groups (**1b**−**1f**) provided the desired products (**3b**−**3f**) in moderate to good yield and excellent enantioselectivity, as did an *ortho*-substituted substrate (**1c**). In addition, substrates bearing a number of functional groups could all be successfully employed to deliver the desired products, including those with an ester (**3d**), a tertiary amide (**3m**), a tertiary arylamine (**3l**), an imide (**3n**), a diaryl ketone (**3t**), and sulfonamides (**3i**, **3u**). Moreover, a variety of heterocycles were well tolerated in this transformation, including benzofurans (**3g**, **3h**), thiophenes (**3j**, **3k**), a pyrrole (**3o**), a carbazole (**3p**), an indole (**3q**), a phenothiazine (**3r**), and a quinoline (**3s**). In all cases examined, the protocol delivered propargylic silanes with excellent levels of stereocontrol (≥95% ee).

Moreover, higher alkyl aryl acetylenes including those possessing pendent functional groups were competent substrates, delivering products **3v**−**3ad** under slightly modified conditions. It was also found that the reaction could selectively undergo propargylic silylation in the presence of a terminal alkene (**3z**). Structurally distinct conjugated enynes (**1ae**−**1ag**) and dialkyl acetylenes (**1ah**−**1aj**) were also successful substrates, delivering products **3ae**−**3aj** in moderate to high yield and good to excellent enantioselectivity (≥80% ee). Remarkably, unsymmetrical acetylenes carrying two primary alkyl substituents (**1ah**, **1ai**) provided silylation products at the less hindered position with synthetically useful regioselectivity (8.3:1 rr and 14:1 rr).

We then investigated the scope of silyl triflate reagents suitable for this transformation. In the case of reagents that were not available commercially (**2bb**−**2bf**), we found that they could be conveniently generated by the protonolysis of the corresponding allyl- or arylsilanes with TfOH and used *in situ* without purification. In all cases examined, propargylic silylation products (**5a**−**5f**) were obtained in moderate to excellent yield and uniformly excellent enantiocontrol (≥94% ee). Notably, a chiral racemic silyl triflate could be used to give **5f** with high levels of enantiocontrol at the propargylic position, though as a mixture of diastereomers at silicon.

In addition, the regioselectivity of propargylsilane formation was examined further by subjecting methyl alkyl acetylenes to the standard reaction conditions (Scheme 3A). In these cases, silylation took place cleanly (>20:1 rr) at the terminal methyl position to give achiral propargylic silanes **6**. Regioselectivity was unaffected by the presence of nitrogen or oxygen substituents on the alkyl chain (**6b**−**6e**). The incorporation of fragments based on bioactive molecules and pharmaceuticals such as fenofibric acid (**6d**), further highlighted the broad scope and functional group compatibility of this silylation protocol.

Table 2 Substrate scope of alkynes and silyl triflates for propargylic silane formation[a]

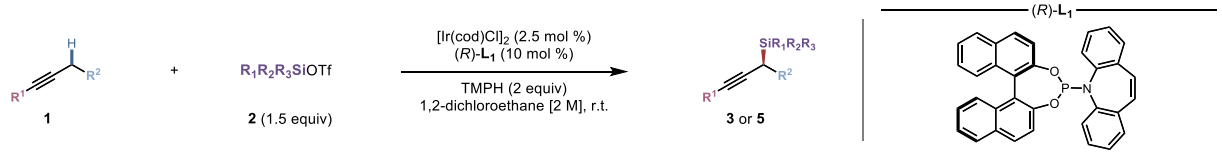

aryl ethyl acetylenes

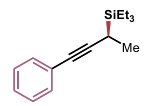

3a
91% *yield*, 97% *ee*

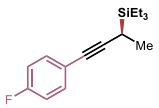

3b
80% *yield*, 97% *ee*

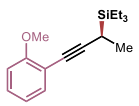

3c
94% *yield*, >99% *ee*

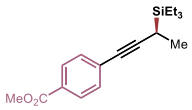

3d
67% *yield*, 97% *ee*

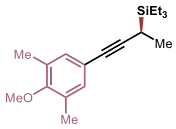

3e
67% *yield*, 96% *ee*

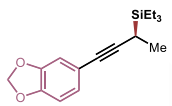

3f
89% *yield*, 98% *ee*

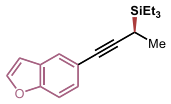

3g
91% *yield*, 96% *ee*

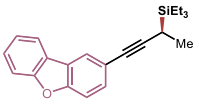

3h
92% *yield*, 97% *ee*

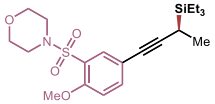

3i
89% *yield*, 95% *ee*

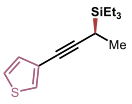

3j
93% *yield*, 97% *ee*

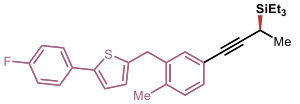

3k *Canagliflozin precusor*
97% *yield*, 97% *ee*

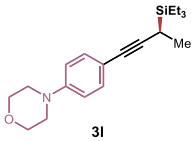

3l
95% *yield*, 97% *ee*
5 mmol : 92% *yield*, 98% *ee*[b]

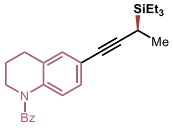

3m
49% *yield*, 97% *ee*

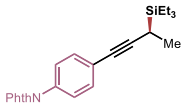

3n
86% *yield*, 97% *ee*

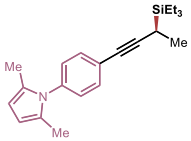

3o
78% *yield*, 98% *ee*

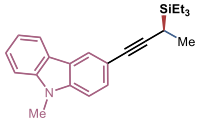

3p
93% *yield*, 97% *ee*

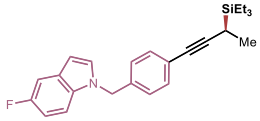

3q
99% *yield*, 95% *ee*

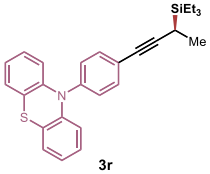

3r
40% *yield*, 96% *ee*

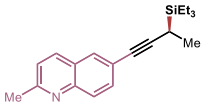

3s
55% *yield*, 94% *ee*

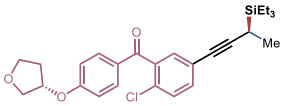

3t *Empagliflozin precusor*
51% *yield*, 98% *de*

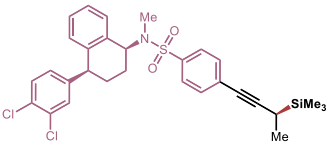

3u *Sertraline derivative*
47% *yield*, 95% *de*

higher alkyl aryl acetylenes

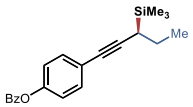

3v
93% *yield*, 98% *ee*

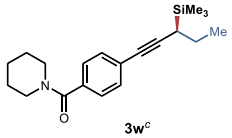

3w[c]
30% *yield*, 95% *ee*

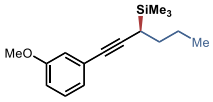

3x[c]
90% *yield*, 96% *ee*

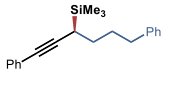

3y[c]
56% *yield*, 92% *ee*

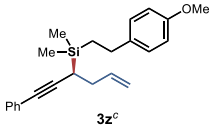

3z[c]
34% *yield*, >99% *ee*

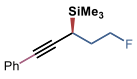

3aa[c]
90% *yield*, 98% *ee*

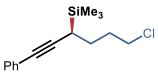

3ab[c]
87% *yield*, 90% *ee*

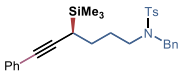

3ac[c]
99% *yield*, 96% *ee*

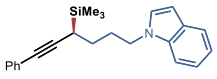

3ad[c]
59% *yield*, 97% *ee*

conjugated enynes

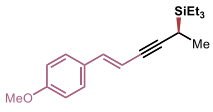

3ae
68% *yield*, 94% *ee*

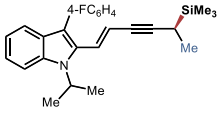

3af[c] *Fluvastatin precusor*
90% *yield*, 98% *ee*

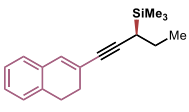

3ag
54% *yield*, 96% *ee*

dialkyl acetylenes

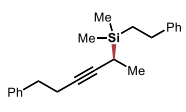

3ah
57% *yield*, 8.3:1 *rr*, 85% *ee*

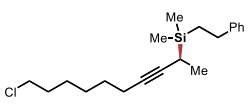

3ai[c]
78% *yield*, 14:1 *rr*, 81% *ee*

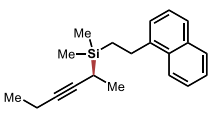

3aj
66% *yield*, 90% *ee*

silyl triflate scope

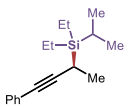

5a[c]
94% *yield*, 88% *ee*

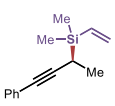

5b
71% *yield*, 98% *ee*

5c
51% *yield*, 97% *ee*
5 mmol : 50% *yield*, 98% *ee*[b]

5d
91% *yield*, 97% *ee*

5e
90% *yield*, 96% *ee*

5f
1.3:1 *dr* *
88% *yield*, ≥94% *ee* (each)

[a] Isolated yields on 0.2 mmol scale. Enantiomeric excesses were determined by HPLC with chiral stationary phase. Regioisomeric ratios were determined by ^{1}H NMR spectroscopy of the crude material. [b] $[Ir(cod)Cl]_2$ (2 mol %) and (*R*)-**L**$_1$ (8 mol %). [c] TMPH (2.5 equiv), silyl triflate (2 equiv), 30 °C.

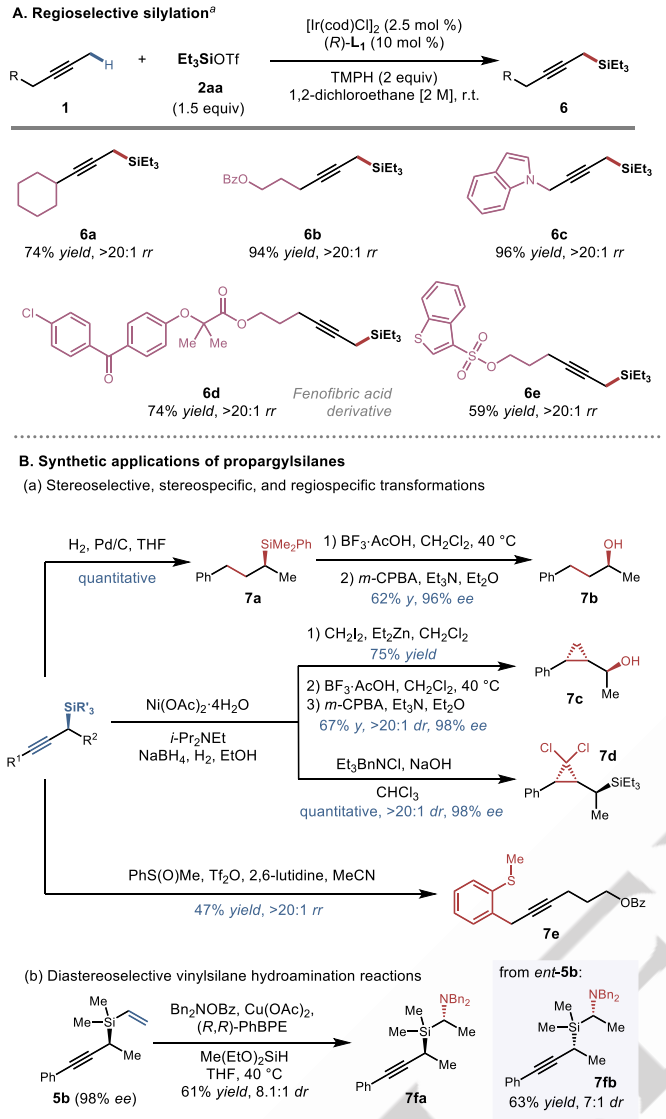

Scheme 3. Substrate scope of regioselective silylation and synthetic applications of silane products [a] Isolated yields on 0.2 mmol scale. Regioisomeric ratios were determined by ^{1}H NMR spectroscopy of the crude material.

The protocol was found to be scalable. On 5 mmol scale, **3l** could be prepared without significant loss in synthetic efficiency or stereoselectivity (1.52 g isolated, 92% yield, 98% ee). In addition, a series of derivatization reactions could be carried out on **3a** and **5c** to deliver products **7b**,[13f] **7c**,[13b] **7d**[13g] with high levels of stereoselectivity, enantiospecificity, and regiospecificity (Scheme 3B, (a)). Notably, comparison of chiral HPLC retention times and optical rotation of **7b** with those reported in the literature allowed the absolute configuration of silane **5c** to be deduced and those of other enantioenriched silane products **3** and **5** to be assigned by analogy. Furthermore, vinyl silanes **5b** and *ent*-**5b** bearing a stereocenter at the propargylic position could undergo CuH-catalyzed hydroamination with catalyst control of diastereoselectivity (Scheme 3B, (b)).[14d]

To gain some insight into the details of this C(sp^3)–H silylation process, we performed a series of experiments to probe the mechanism of this iridium-catalyzed process. We began by examining the kinetic isotope effect using 1-phenyl-1-butyne (**1a**) and its deuterated isotopologue (**1a**-d_5). Initial experiments conducted in an intermolecular competition experiment resulted in a KIE value of 7.86±0.29 with TMSOTf as the silylation reagent. Under similar conditions, the use of TESOTf yielded a smaller KIE value of 2.49±0.38 (Scheme 4A). While the large primary kinetic isotope effect in the experiment with TMSOTf implies an irreversible and turnover limiting proton abstraction step, the smaller KIE value for the experiment with TESOTf indicates that deprotonation, together with a subsequent step (likely C–Si bond formation), are partially rate-determining with this larger electrophile.[22]

To probe the nature of the stereocontrol of this transformation, we investigated the relationship between the enantiomeric excess of the catalyst and the enantiomeric composition of the product. Firstly, when scalemic catalyst mixtures were prepared by mixing the preformed [(*R*)-**L$_1$**]$_2$IrCl and [(*S*)-**L$_1$**]$_2$IrCl catalysts, a linear correlation between the catalyst ee and product ee was observed. In contrast, when the scalemic catalyst mixtures were prepared by mixing appropriate amounts of antipodal ligands (*R*)- and (*S*)-**L$_1$** *before* combining with [Ir(cod)Cl]$_2$, a strong positive non-linear effect was observed (Scheme 4B). These results indicate that (**L$_1$**)$_2$Ir$^+$ species are likely involved in catalysis and that the catalytically active species carrying two homochiral phosphoramidite ligands do not exchange these ligands under the reaction conditions.[23]

We then sought to determine the kinetic order of each of the reagents and the catalyst by varying the concentrations of each component (alkyne **1a**, [Ir]/**L$_1$** (Ir : **L$_1$** = 1:2), TMPH, and TESOTf) and measuring initial rates of reaction to provide silylation product **3a**. These experiments revealed approximately first-order dependence on catalyst, base, and silyl triflate but zero order dependence on the alkyne (Scheme 4C). Stoichiometric NMR experiments demonstrate that, in the presence of alkyne, silyl triflate reagents abstracts Cl^- completely from the phosphoramidite-ligated Ir center within 10 min to generate the cationic alkyne complex **II** (see the Supporting Information).[24] Moreover, ^{31}P NMR analysis of the reaction mixture indicates that **II** is the major phosphorus-containing species during the course of the reaction (up to 50% conversion). These observations suggest that complex **II** is the catalyst resting state and are consistent with the zero order kinetic dependence on [**1a**].

Based on these experimental observations and inferences, we proposed three major possible pathways in Figure 1A. Initially, upon addition of silyl triflate and alkyne into a catalyst mixture containing Ir[(*R*)-**L$_1$**]$_2$Cl (**I**), complex **II** is generated by halide abstraction and alkyne coordination. In the non-redox pathway (a), the direct deprotonation of complex **II** affords the allenyliridium intermediate (η^1 or η^3) **III**, which undergoes outer-sphere attack by the electrophilic silylation reagent to give the propargylic functionalized product **3a**. Alternatively, the intermediate **III** could undergo sucessive electrophilic addition of silyl triflate[25] to the Ir center to give Ir(III) complex **VIII**, which subsequently undergoes reductive elimination to afford **3a** (pathway (b)). In another possible pathway (c), oxidative addition of the silyl triflate to the Ir center of complex **V** followed by coordination of alkyne gives dicationic Ir(III) species **VII**.[26] Subsequent propargylic

deprotonation of **VII** affords **VIII**, which then undergoes C–Si bond-forming reductive elimination on the Ir center to regenerate the Ir(I) catalyst as coordinatively unsaturated species **V**. Since these pathways could all account for observed rate law, we turned to computations to gain insight into their feasibility.

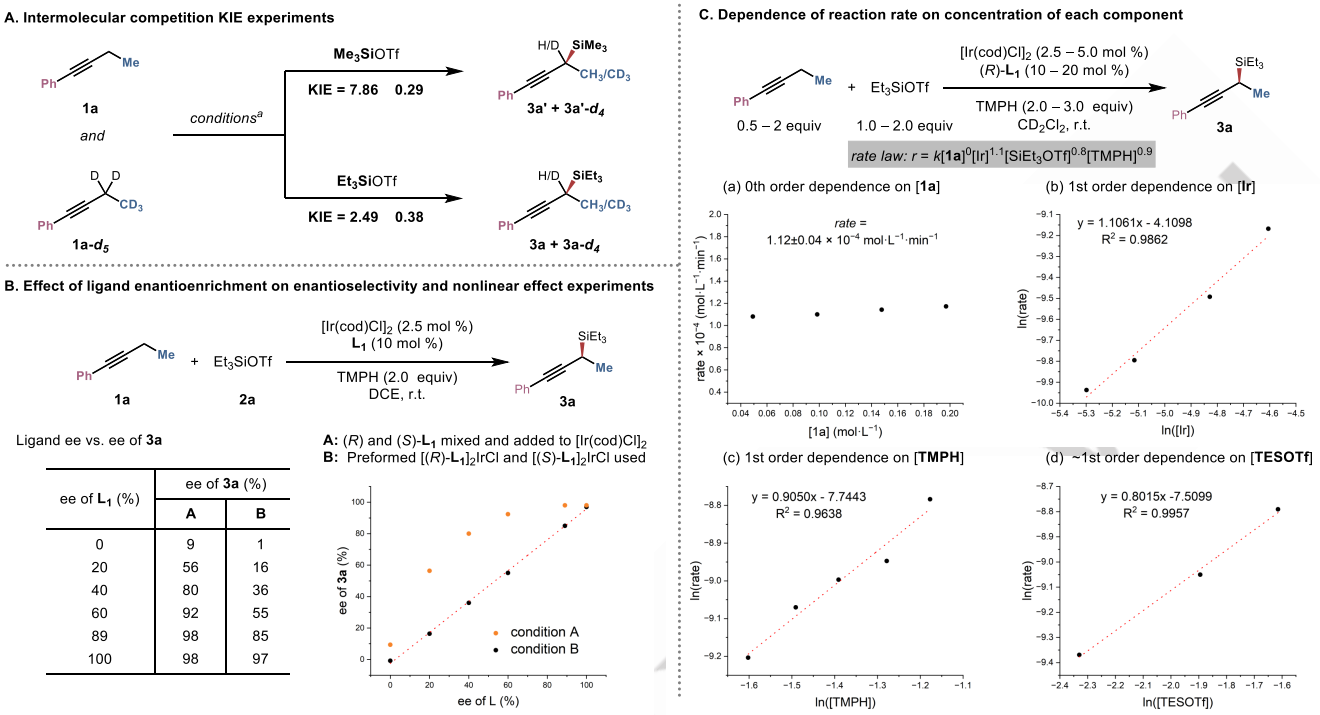

Scheme 4. Experimental mechanistic studies on the Ir-catalyzed propargylic silylation reaction. [a] Reaction conditions: **1a** (0.1 mmol), **1a**-d_5 (0.1 mmol), $[Ir(cod)Cl]_2$ (2.5 mol %) and (*R*)-$\mathbf{L_1}$ (10 mol %), TMSOTf or TESOTf (1.5 equiv), TMPH (2 equiv), 1,2-dichloroethane (0.1 mL).

We performed density functional theory (DFT) calculations to investigate the three proposed mechanisms of the Ir-catalyzed silylation and factors that control the enantioselectivity. The calculations were performed using 1-phenyl-1-butyne (**1a**) as the model alkyne substrate and TMSOTf as the silylation reagent. Our calculations indicate that pathway (a) is the most favorable pathway (Figure 1B). From the cationic π-alkyne Ir(I) complex **8** supported by two phosphoramidite ligands (*R*)-$\mathbf{L_1}$, deprotonation of the propargylic C–H bond by TMPH[10, 27] occurs via an outer-sphere transition state (**TS1**) with an activation free energy of 27.3 kcal/mol with respect to **8**. This process leads to an η^3-propargyl/allenyl complex **9**.[28] Subsequent outer-sphere attack of TMSOTf[29] takes place via **TS2**, which directly leads to the π complex (**10**) carrying the coordinated propargylic silylation product. Subsequent alkyne ligand exchange releases product (*S*)-**3a'** and regenerates reactant complex **8**. When the TMSOTf electrophile was used, the deprotonation (**TS1**) is the rate-determining step because it requires a higher barrier than silylation (**TS2**). However, when the bulkier TESOTf is used, the silyl addition is predicted to have a higher Gibbs free energy than deprotonation ($\Delta G^{\ddagger}$ = 30.8 and 27.3 kcal/mol, respectively, with respect to **8**) and comparable enthalpy ($\Delta H^{\ddagger}$ = 13.5 and 13.1 kcal/mol, respectively) (Figure 1D). These computational results are consistent with the KIE experiments that suggested a potential change of rate-determining step when bulkier electrophiles were used (Scheme 4A). Pathways (b) and (c) were found to be less favorable than pathway (a) (Figure 1C and Figure S2 and S3 in the Supporting Information). The transition state for the oxidative addition of TMSOTf to neutral Ir complex **9** (**TS3**, $\Delta G^{\ddagger}$ = 50.3 kcal/mol, pathway (b)) and for the oxidative addition following initial alkyne displacement for cationic Ir complex **8** (**TS4**, $\Delta G^{\ddagger}$ = 41.3 kcal/mol, pathway (c)) both require much higher energy than the rate-determining C–H deprotonation in pathway (a). These results reveal that the direct outer-sphere silyl addition to η^3-propargyl/allenyl complex **9** is more favorable than pathways involving oxidative addition of silyl triflate to the Ir center.

Next, we explored the origin of enantioselectivity by comparing the C–H deprotonation/silyl addition pathways leading to both enantiomers of the silylation products (Figure 1E, see Figure S1 in the Supporting Information for the complete reaction energy profiles). The calculations indicate that the silyl addition transition state **TS2** that leads to the experimentally observed enantiomer (*S*)-**3a'** is 7.1 kcal/mol more stable than **TS2'**, which leads to the minor enantiomer (*R*)-**3a'**. Here, **TS2'** is destabilized by steric repulsions between the propargylic methyl substituent and the phosphoramidite ligands. Distortion energy calculations (see Table S2 in the Supporting Information) indicate that both the Ir catalyst and alkyne substrate are more distorted in **TS2'** than in **TS2** due the ligand–substrate steric repulsions. By contrast, in the more favorable silylation transition state isomer **TS2**, a

propargylic C–H bond points towards the phosphoramidite ligands, instead of the bulkier methyl group, leading to diminished ligand–substrate steric interactions while enabling stabilizing π/π interactions between the two phosphoramidite ligands.

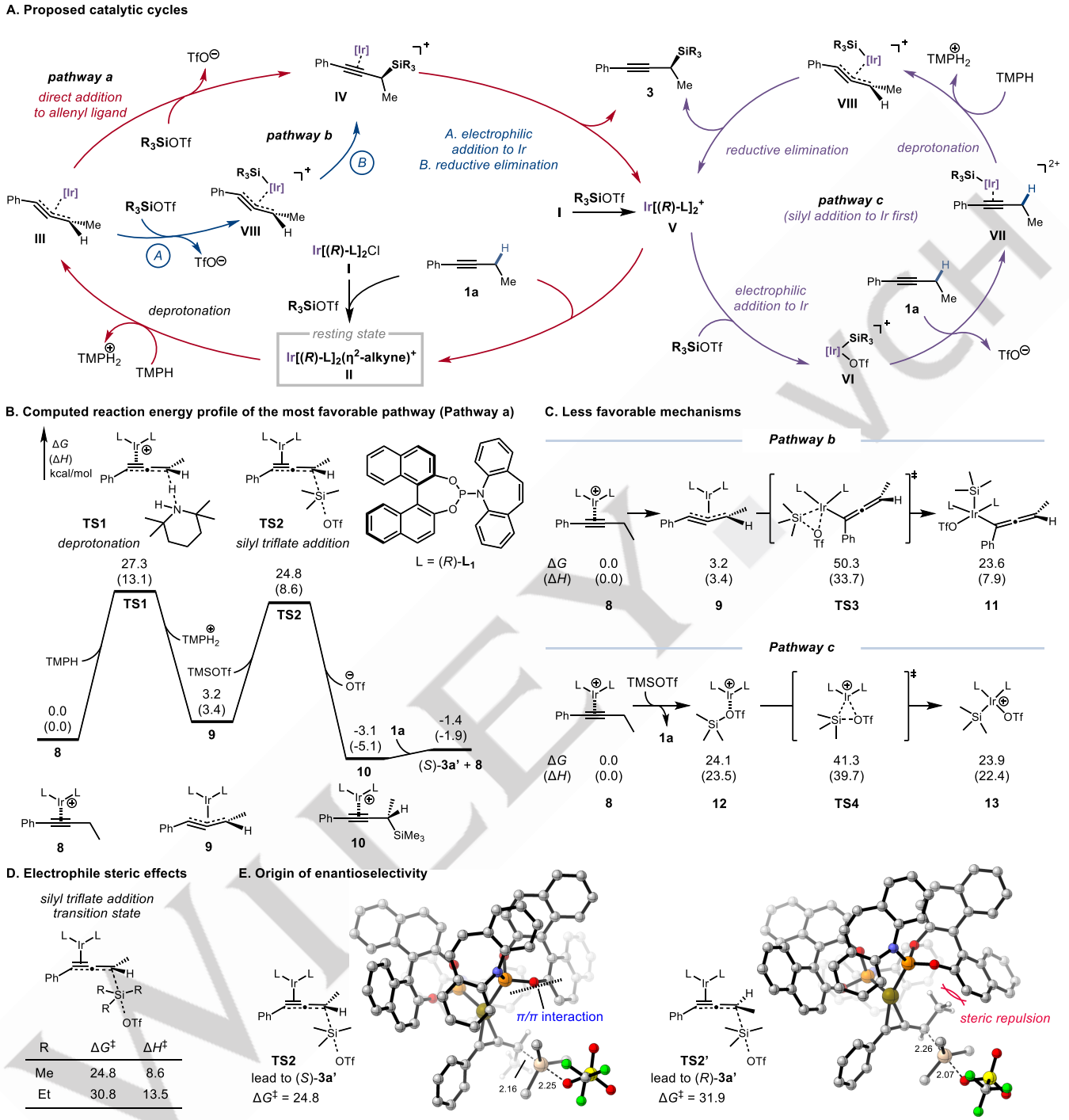

R	ΔG‡	ΔH‡
Me	24.8	8.6
Et	30.8	13.5

Figure 1. Plausible pathways and computational studies. DFT calculations were performed at the ωB97x-D/SDD(Ir)–6-311+G(d,p)/SMD(DCE)//B3LYP-D3(BJ)/SDD(Ir)–6-31G(d) level of theory. All energies are in kcal/mol. Bond distances are given in Å.

In addition to these synthetic and mechanistic studies on the preparation of propargylsilanes, we further examined the generality of the synthesis of allenylsilanes using reaction conditions employing silyl bistriflimides (Scheme 5A). A collection of alkynes was first investigated. A range of alkynes bearing electron neutral or electron withdrawing groups was found to afford the allenylsilane products with moderate to very high levels of regioselectivity and excellent levels of enantioselectivity (**4aa**, **4b**-**4i**). X-ray crystallographic analysis of compound **4h** was conducted to ascertain the absolute configuration of the major enantiomer and allow the remainder to be assigned by analogy.[30] Moreover, two non-commercial silyl bistriflimides were prepared *in situ* as silylation reagents, allowing for the synthesis of **4j** and **4k** in synthetic useful yields and excellent enantioselectivities,

regardless of the silane substituents employed. The enantioenriched allenylsilanes could be employed in Sakurai reactions with aldehyde or iminium electrophiles, providing the homopropargylic addition products **7g**[13i] and **7h**[13j] with excellent transfer of chirality (Scheme 5B).

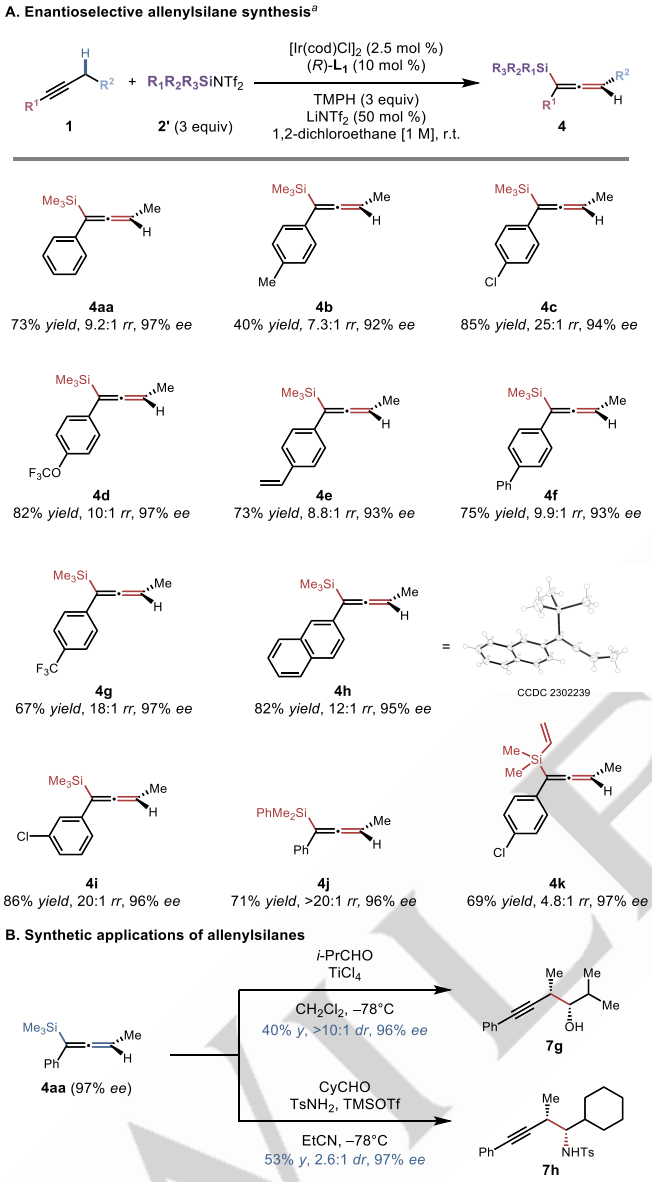

Scheme 5. Synthesis of allenylsilanes and their synthetic applications. [a] Isolated yields on 0.2 mmol scale. Regioisomeric and diastereomeric ratios were determined by ^{1}H NMR spectroscopy of the crude material. Enantiomeric excesses were determined by HPLC with chiral stationary phase.

Conclusion

In summary, we developed a direct enantioselective propargylic silylation of alkynes. This method features high enantio- and regioselectivity, and a catalytic cycle was proposed involving outer-sphere attack of silyl triflate reagent by an η^3-propargyl/allenyl Ir species, based on experimental and computational mechanistic data. Further studies of the detailed mechanism and explorations of additional applications of this strategy toward installation of propargylic stereocenters are ongoing and will be reported in due course.

Acknowledgements

We gratefully acknowledge support from the University of Pittsburgh for startup funding. Research reported in this publication was also supported by the National Institute of General Medical Sciences, National Institutes of Health (R35GM142945, Y.-M.W.) and the National Science Foundation (CHE-2247505, P.L.). J.Z. gratefully acknowledges the Dietrich School of Arts and Sciences, University of Pittsburgh for an Andrew Mellon Predoctoral Fellowship. We thank Professor John Hartwig (UC Berkeley) for helpful discussions on the mechanism. We thank Professor Kay Brummond (Pittsburgh) for sharing HPLC resources. We thank Yifan Qi (Brummond research group) for extensive assistance in the collection of normal-phase HPLC data and Sarah Scrivener for assistance with reverse-phase HPLC for silane **3q**. DFT calculations were carried out at the University of Pittsburgh Center for Research Computing and the Advanced Cyberinfrastructure Coordination Ecosystem: Services & Support (ACCESS) program, supported by NSF award numbers OAC-2117681, OAC-1928147 and OAC-1928224.

Keywords: C–H functionalization • enantioselective silylation • propargylic • allenic • DFT calculations

[1] (a) K. Lauder, A. Toscani, N. Scalacci, D. Castagnolo, *Chem. Rev.* **2017**, *117*, 14091. (b) F. T. Zindo, J. Joubert, S. F. Malan, *Future Med. Chem.* **2015**, *7*, 609. (c) Y. Zheng, L. Zhang, E. Meggers, *Org. Process Res. Dev*. **2018**, *22*, 103.

[2] (a) J. Cossy, A. Schmitt, C. Cinquin, D. Buisson, D. Belotti, *Chem. Lett.* **1997**, *7*, 1699. (b) H.-N. Zou, Y.-T. Zhao, L.-L. Yang, M.-Y. Huang, J.-W. Zhang, M.-L. Huang, S.-F. Zhu, *ACS Catal.* **2022**, *12*. (c) T. Brodmann, D. Janssen, M. Kalesse, *J. Am. Chem. Soc.* **2010**, *132*, 13610. (d) A. Fürstner, E. Kattnig, O. Lepage, *J. Am. Chem. Soc.* **2006**, *128*, 9194.

[3] Reviews: (a) C.-H. Ding, X.-L. Hou, *Chem. Rev.* **2011**, *111*, 1914. (b) Y. Nishibayashi, *Synthesis* **2012**, *44*, 489. (c) D.-Y. Zhang, X.-P. Hu, *Tetrahedron Lett.* **2015**, *56*, 283. (d) Y. Sempere, E. M. Carreira, *Organic Reactions*. **2022**, 207.

[4] (a) L. X. Alvarez, M. L. Christ, A. B. Sorokin, *Appl. Catal. A: Gen.* **2007**, *325*, 303. (b) J. S. Clark, K. F. Tolhurst, M. Taylor, S. Swallow, *Tetrahedron Lett.* **1998**, *39*, 4913. (c) J. Xi, X. Zhu, H. Bao, *Synthesis.* **2024**, DOI:10.1055/a-2240-5349.

[5] Y. Deng, R. Lu, P. Chen, G. Liu, *Chem. Commun*., **2023**, *59*, 4656.

[6] R. Lu, T. Yang, X. Chen, W. Fan, P. Chen, Z. Lin, G. Liu, *J. Am. Chem. Soc.* **2021**, *143*, 14451.

[7] (a) M. Ju, E. E. Zerull, J. M. Roberts, M. Huang, I. A. Guzei, J. M. Schomaker, *J. Am. Chem. Soc.* **2020**, *142*, 12930. (b) H. Wang, Y. Park, Z. Bai, S. Chang, G. He, G. Chen, *J. Am. Chem. Soc.* **2019**, *141*, 7194. (c) P. Xu, J.-J. Xie, D.-S. Wang, X. P. Zhang, *Nat. Chem.* **2023**, *15*, 498. (d) Y. Yamakawa, T. Ikuta, H. Hayashi, K. Hashimoto, R. Fujii, K. Kawashima, S. Mori, T. Uchida, R. Katsuki, *J. Org. Chem.* **2022**, *87*, 6769.

[8] (a) Z. Liu, Z.-Y. Qin, L. Zhu, S. V. Athavale, A. Sengupta, Z.-J. Jia, M. Garcia-Borràs, K. N. Houk, F. H. Arnold, *J. Am. Chem. Soc.* **2022**, *144*, 80. (b) S. Hu, L. P. Hager, *J. Am. Chem. Soc.* **1999**, *121*, 872.

[9] (a) T. Li, L. Zhang, *J. Am. Chem. Soc.* **2018**, *140*, 17439. (b) Z. Wang, Y. Wang, L. Zhang, *J. Am. Chem. Soc.* **2014**, *136*, 8887. (c) Y. Wang, J. Zhu, A. C. Durham, H. Lindberg, Y.-M. Wang, *J. Am. Chem. Soc.* **2019**, *141*, 19594. (d) Y. Wang, J. Zhu, R. Guo, H. Lindberg, Y.-M. Wang, *Chem. Sci.* **2020**, *11*, 12316. (e) K. L. Gutman, C. D. Quintanilla, L. Zhang, *J. Am. Chem. Soc.* **2024**, DOI: 10.1021/jacs.3c11919.

[10] T. Li, X. Cheng, P. Qian, L. Zhang, *Nat. Catal.* **2021**, *4*, 164.

[11] J. Zhu, Y. Wang, A. D. Charlack, Y.-M. Wang, *J. Am. Chem. Soc.* **2022**, *144*, 15480.

[12] (a) M. A. Brook, *Silicon in Organic, Organometallic, and Polymer Chemistry*, Wiley–Interscience, New York, **2000**. (b) E. Langkopf, D. Schinzer, *Chem. Rev.* **1995**, *95*, 1375. (c) A. K. Franz, S. O. Wilson, *J. Med. Chem.* **2013**, *56*, 388. (e) S. B. J. Kan, R. D. Lewis, K. Chen, F. H. Arnold, *Science* **2016**, *354*, 1048.

[13] (a) T. H. Chan, D. Wang, *Chem. Rev.* **1992**, *92*, 995. (b) I. Fleming, R. Henning, H. Plaut, *J. Chem. Soc., Chem. Commun*. **1984**, 29. (c) D. A. Evans, Y. Aye, *J. Am. Chem. Soc.* **2007**, *129*, 9606. (d) S. Yu, S. Ma, *Angew. Chem., Int. Ed.* **2012**, *51*, 3074. (e) M. J. C. Buckle, I. Fleming, S. Gil, K. L. C. Pang, *Org. Biomol. Chem*. **2004**, *2*, 749. (f) P. J. Murphy, J. L. Spencer, G. Procter, *Tetrahedron Lett.* **1990**, *31*, 1055. (g) J. M. Adam, L. de Fays, M. Laguerre, L. Ghosez, *Tetrahedron* **2004**, *60*, 7325. (h) A. J. Eberhart, H. Shrives, E. Álvarez, A. Carrër, Y. Zhang, D. J. Procter, *Chem. - Eur. J.* **2015**, *21*, 7428. (i) M. J. C. Buckle, I. Fleming, *Tetrahedron Lett.* **1993**, *34*, 2383. (j) R. A. Brawn, J. S. Panek, *Org. Lett.* **2009**, *11*, 4362.

[14] (a) C. Walter, M. Oestreich, *Angew. Chem., Int. Ed.* **2008**, *47*, 3818. (b) K.-S. Lee, A. H. Hoveyda, *J. Am. Chem. Soc.* **2010**, *132*, 2898. (c) T. Ohmura, H. Taniguchi, Y. Kondo, M. Suginome, *J. Am. Chem. Soc.* **2007**, *129*, 3518. (d) M. W. Gribble, M. T. Pirnot, J. S. Bandar, R. Y. Liu, S. L. Buchwald, *J. Am. Chem. Soc.* **2017**, *139*, 2192. (e) W.-W. Zhang, B.-J. Li, *Angew. Chem., Int. Ed.* **2022**, *62*, e202214534. (f) L. B. Delvos, D. J. Vyas, M. Oestreich, *Angew. Chem. Int. Ed.* **2013**, *52*, 4650. (g) H. Yi, W. Mao, M. Oestreich, *Angew. Chem., Int. Ed.* **2019**, *58*, 3575. (h) J. L. Hofstra, A. H. Cherney, C. M. Ordner, S. E. Reisman, *J. Am. Chem. Soc.* **2018**, *140*, 139. (i) R. D. Lewis, M. Garcia-Borràs, M. J. Chalkley, A. R. Buller, K. N. Houk, S. B. J. Kan, F. H. Arnold, *Proc. Natl. Acad. Sci. U. S. A.* **2018**, *115*, 7308. (j) L.-L. Yang, D. Evans, B. Xu, W.-T. Li, M.-L. Li, S.-F. Zhu, K. N. Houk, Q.-L. Zhou, *J. Am. Chem. Soc.* **2020**, *142*, 12394. (k) B. Yang, K. Cao, G. Zhao, J. Yang, J. Zhang, *J. Am. Chem. Soc.* **2022**, *144*, 15468. (l) Y. Yasutomi, H. Suematsu, T. Katsuki, *J. Am. Chem. Soc.* **2010**, *132*, 4510.

[15] Enantioselective propargylsilane synthesis: (a) L.-L. Yang, J. Ouyang, H.-N. Zou, S.-F. Zhu, Q.-L. Zhou, *J. Am. Chem. Soc.* **2021**, *143*, 6401. (b) W. Mao, M. Oestreich, *Org. Lett.* **2020**, *22*, 8096. Enantioselective allenylsilane synthesis: (c) J. W. Han, N. Tokunaga, T. Hayashi, *J. Am. Chem. Soc.* **2001**, *123*, 12915. (d) M, Wang, Z.-L. Liu, X. Zhang, P.-P. Tian, Y.-H. Xu, T.-P. Loh, *J. Am. Chem. Soc.* **2015**, *137*, 14830. (e) Z. -L. Liu, C. Yang, Q.-Y. Xue, M. Zhao, C.-C. Shan, Y.-H. Xu, T.-P. Loh, *Angew. Chem., Int. Ed.* **2019**, *58*, 16538. (f) T. J. O'Connor, B. K. Mai, J. Nafie, P. Liu, F. D. Toste, *J. Am. Chem. Soc.* **2021**, *143*, 13759. (g) C. Jin, X. He, S. Chen, Z. Guo, Y. Lan, X. Shen, *Chem*, **2023**, *9*, 1. (h) Z.-L. Wang, Q. Li, M.-W. Yang, Z.-X. Song, Z.-Y. Xiao, W.-W Ma, J.-B. Zhao, Y.-H. Xu, *Nat. Commun*. **2023**, *14*, 1.

[16] (a) M. Oestreich, *Synlett* **2007**, *2007*, 1629. (b) Y. Ge, X. Huang, J. Ke, C. He, *Chem. Catal.* **2022**, *2*, 2898. (c) B. Su, J. F. Hartwig, *Angew. Chem., Int. Ed*. **2022**, *61*, e202113343.

[17] Reviews: (a) C. Cheng, J. F. Hartwig, *Chem. Rev.* **2015**, *115*, 8946. Recent examples: (b) X.-H. Zhou, J.-H. Zhu, G.-A. Song, X.-L. Jiang, X.-J. Fang, Z. Xu, L.-W. Xu, *Org. Chem. Front.*, **2023**, *10*, 5443. (c) J. W. Wilson, B. Su, M. Yoritate, J. X. Shi, and J. F. Hartwig, *J. Am. Chem. Soc.* **2023**, 145, 19490.

[18] (a) T. Lee, J. F. Hartwig, *Angew. Chem. Int. Ed* **2016**, *55*, 8723. (b) B. Su, J. F. Hartwig, *J. Am. Chem. Soc.* **2017**, *139*, 12137. (c) B. Su, T. Lee, J. F. Hartwig, *J. Am. Chem. Soc.* **2018**, *140*, 18032. (d) B. Yang, W. Yang, Y. Guo, L. You, C. He, *Angew. Chem., Int. Ed.* **2020**, *59*, 22217. (e) Y. Guo, M.-M. Liu, X. Zhu, L. Zhu, C. He, *Angew. Chem., Int. Ed.* **2021**, *60*, 13887. (f) M. Murai, H. Takeshima, H. Morita, Y. Kuninobu, K. Takai, *J. Org. Chem.* **2015**, *80*, 5407.

[19] Review: (a) K. M. Korch, D. A. Watson, *Chem. Rev.* **2019**, *119*, 8192. (b) Y.-H. Yang, X. Pang, X.-Z. Shu, *Synthesis* **2023**, *55*, 868. (c) X. Pang, X.-Z. Shu, *Chem. Eur. J.* **2023**, *29*, e202203362. Selected examples: (d) B. Vulovic, A. P. Cinderella, D. A. Watson, *ACS Catal.* **2017**, *7*, 8113. (e) A. P. Cinderella, B. Vulovic, D. A. Watson, *J. Am. Chem. Soc.* **2017**, *139*, 7741. (f) L. Zhang, M. Oestreich, *Angew. Chem., Int. Ed.* **2021**, *60*, 18587. (g) L. Qi, Q.-Q. Pan, X.-X. Wei, X. Pang, Z. Liu, X.-Z. Shu, *J. Am. Chem. Soc.* **2023**, *145*, 13008.

[20] J. R. McAtee, S. E. Martin, A. P. Cinderella, W. B. Reid, K. A. Johnson, D. A. Watson, *Tetrahedron* **2014**, *70*, 4250.

[21] (a) W. Uhlig, *Prog. Polym. Sci.* **2002**, *27*, 255. (b) W. Uhlig, *J. Organomet. Chem.***1993**, *452*, 29.

[22] (a) Y. Xia, G. Lu, P. Liu, G. Dong. *Nature* **2016**, *539*, 546. (b) C. Cheng, J. F. Hartwig, *J. Am. Chem. Soc.* **2014**, *136*, 12064.

[23] Y. Motoyama, M. Terada, K. Mikami, *J. Am. Chem. Soc.* **1994**, *116*, 2812.

[24] E.A. Standley, T. F. Jamison, *J. Am. Chem. Soc.* **2013**, *135*, 1585.

[25] (a) A. A. Zlota, F. Frolow, D. Milstein, *J. Chem. Soc., Chem. Commun.* **1989**, *0*, 1826. (b) H. Yamashita, A. M. Kawamoto, M. Tanaka, M. Goto, *Chem. Lett*. **1990**, *19*, 2107.

[26] (a) B. P. Cleary, R. Eisenberg, *Inorg. Chim. Acta* **1995**, *240*, 135. (b) M. Janka, W. He, W.A. J. Frontier, R. Eisenberg, *J. Am. Chem. Soc.* **2004**, *126*, 6864.

[27] (a) R. Wang, Y. Wang, R. Ding, P. B. Staub, C. Z. Zhao, P. Liu, Y.-M. Wang, *Angew. Chem., Int. Ed.* **2023**, *62*, e202216309. (b) B. Wu, H. Z. Su, Z. Y. Wang, Z. D. Yu, H. L. Sun, F. Yang, J. H. Dou, R. Zhu, *J. Am. Chem. Soc.* **2022**, *144*, 4315. (c) L. Zheng, Z. Yan, Q. Ren, *Appl. Organomet. Chem.* **2022**, 36, e6549. (d) K. Zhong, C. Shan, L. Zhu, S. Liu, T. Zhang, F. Liu, B. Shen, Y. Lan, R. Bai, *J. Am. Chem. Soc.* **2019**, *141*, 5772.

[28] (a) J. Zhao, Y. Liu, Q. He, Y. Li, S. Ma, *Chem. Eur. J.* **2009**, *15*, 11361. (b) M. Fortunato, Y. Gimbert, E. Rousset, P. Lameiras, A. Martinez, S. Gatard, R. Plantier-Royon, F. Jaroschik, *J. Org. Chem*. **2020**, *85*, 10681. (c) Y.-C. Cheng, Y.-K. Chen, T.-M. Huang, C.-I. Yu, G.-H. Lee, Y. Wang, J.-T. Chen, J.-T. *Organometallics* **1998**, *17*, 2953. (d) H. Nagae, A. Kundu, H. Tsurugi, K. Mashima, *Organometallics* **2017**, *36*, 3061. (e) M. D. Aparece, W. Hu, J. P. Morken, *ACS Catal*. **2019**, *9*, 11381.

[29] A. Glüer, J. I. Schweizer, U. S. Karaca, C. Würtele, M. Diefenbach, M. C. Holthausen, S. Schneider, *Inorg. Chem*. **2018**, *57*, 13822.

[30] Deposition Number(s) <url href="https://www.ccdc.cam.ac.uk/services/structures?id=doi:10.1002/anie.202318040"> 2302239 (for **4h**)</url> contain(s) the supplementary crystallographic data for this paper. These data are provided free of

charge by the joint Cambridge Crystallographic Data Centre and Fachinformationszentrum Karlsruhe <url href="http://www.ccdc.cam.ac.uk/structures">Access Structures service</url>.

Entry for the Table of Contents

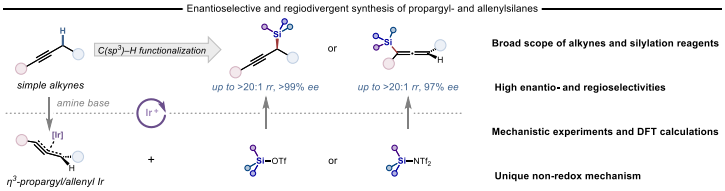

We report a highly enantioselective intermolecular propargylic C−H silylation mediated by a η^3-propargyl/allenyl Ir complex. Under reagent-controlled protocols, propargylsilanes resulting from C(sp^3)−H functionalization, as well the regioisomeric, synthetically versatile allenylsilanes, could be obtained with excellent levels of enantioselectivity and good to excellent control of propargyl/allenyl selectivity.